ELSEVIER

J. Non-Newtonian Fluid Mech. 139 (2006) 44–53

Journal of Non-Newtonian Fluid Mechanics

www.elsevier.com/locate/jnnfm

Constitutive modeling and flow simulation of polytetrafluoroethylene (PTFE) paste extrusion

Pramod D. Patil, James J. Feng, Savvas G. Hatzikiriakos *

Department of Chemical and Biological Engineering, The University of British Columbia, 2360 East Mall, Vancouver, BC V6T 1Z3, Canada

Received 14 September 2005; received in revised form 29 January 2006; accepted 28 May 2006

Abstract

A constitutive rheological equation is proposed for the paste extrusion of polytetrafluoroethylene (PTFE) that takes into account the continuous change of the microstructure during flow, through fibril formation. The mechanism of fibrillation is captured through a microscopic model for a structural parameter, ξ. This model essentially represents a balance of fibrillated and unfibrillated domains in the PTFE paste through a first-order kinetic differential equation. The rate of fibril formation is assumed to be a function of the strain rate and a flow type parameter, which describes the relative strength of straining and rotation in mixed type flows. The proposed constitutive equation consists of a shear-thinning and a shear-thickening terms, the relative contribution of the two being a function of ξ. Finite element simulations using the proposed constitutive relation predict accurately the variations of the extrusion pressure with the apparent shear rate and die geometrical parameters.

Keywords: Polytetrafluoroethylene; Paste extrusion; Fibrillation; Structural parameter; Flow type parameter; Finite element simulations

1. Introduction

Owing to its high melting point and melt viscosity, it becomes almost impossible to melt-process polytetrafluoroethylene (PTFE) [1–4]. Instead, techniques involving cold processing, paste extrusion and sintering have to be employed. In PTFE paste extrusion that is of interest to the present work, fine powder of the PTFE resin (primary particle diameter of approximately 0.20 μm) is first mixed thoroughly with a lubricating liquid to form a paste. The paste is consequently extruded through a conical die at a low temperature, typically 35 °C. A schematic diagram of the die used to process the PTFE paste is shown in Fig. 1. It consists of two parts: (i) the die entry, the region where mixed shear and extensional deformation occurs and (ii) the die land that is a capillary of constant cross-section attached at the bottom of the conical section of the die. The die is attached at the bottom of a capillary rheometer. Due to the presence of the lubricant, slippage of the paste at the solid boundaries of the die is possible and the flow is rather complicated.

The conical die entry shown in Fig. 1 is defined by the entry angle (2α), an important parameter in paste extrusion; the reduction ratio, RR, defined as the ratio of the initial to the final cross-sectional area of the conical entry, D_b^2/D^2; and the length-to-diameter ratio, L/D. During the PTFE paste extrusion through such a die, complex structural changes occur in the polymer paste that significantly influence its rheology. These structural changes have been determined by scanning electron microscopy (SEM) analysis [2,5]. Fig. 2 shows typical SEM micrographs of the paste before, during and after the extrusion. The most remarkable feature is the formation of fibrils between neighboring polymer particles. This is due to the mechanical interlocking of crystallites of neighboring particles which unwind as the particles enter the converging conical die (extensional flow) [2,5–9]. Fig. 2a shows the absence of fibrils in the unprocessed paste, where PTFE particles essentially retain their spherical identity. Fig. 2b shows the existence of fibrils as the paste flows downstream in the conical die zone. At the exit of the die and depending on the geometrical characteristics of the die, the paste might become nearly fully fibrillated (Fig. 2c). It is these submicron-diameter fibrils between polymer particles that essentially give the dimensional stability and strength to the final extruded product.

The experimental dependence of extrusion pressure on reduction ratio (RR), entrance angle (2α) and die land L/D ratio of conical dies has been studied for several types of PTFE and lubricants [4,7,8]. A somewhat unexpected observation is that the

* Corresponding author. Tel.: +1 604 822 3107; fax: +1 604 822 6003.
E-mail address: hatzikir@interchange.ubc.ca (S.G. Hatzikiriakos).

0377-0257/$ – see front matter © 2006 Elsevier B.V. All rights reserved.
doi:10.1016/j.jnnfm.2006.05.013

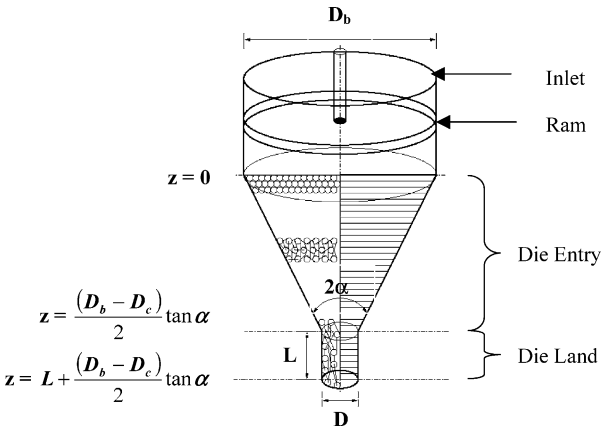

Fig. 1. A conical entry die used in the paste extrusion of PTFE. The left half illustrates the extrusion of PTFE particles and the gradual structure formation through particle fibrillation, whereas the shaded area depicts the axisymmetric domain used in the simulations.

extrusion pressure varies non-monotonically with the entrance angle of the conical die; 2α, and it achieves a minimum for an intermediate entrance angle, $2\alpha \approx 30^\circ$. It has also been recognized that the rheological behavior of PTFE pastes is strongly dependent on the number of fibrils formed between PTFE particles during the extrusion. This implies that the rheology of the paste continuously changes and this complicates the flow modeling. The formation of fibrils has not been given any consideration in previous models [7,8,11,12], and it is the main focus of the present study. Furthermore, experiments have shown that the degree of fibrillation depends on the operating parameters as well as design characteristics of the die [4,7,8]. Therefore, a rational approach seems to be to first formulate an approximate rheological constitutive equation that takes into account the structure formation through fibrillation; and then to use this equation to simulate the paste extrusion process and compare the calculated with the experimental extrusion pressure, as a function of operating and die geometrical characteristics.

In this paper, first a constitutive equation is proposed based on the concept of a structural parameter, ξ. This parameter represents the percentage of the domains of the PTFE material that are fibrillated and takes values of 0 and 1 for the unfibrillated and fully fibrillated cases, respectively. The evolution of the structural parameter is described by a first-order kinetic differential equation, which is developed based on concepts borrowed from network theory of polymeric liquids [13–16]. Similar concepts have been adopted in studies of the rheology of filled polymers and dilute polymer solutions [17,18]. The constitutive equation is subsequently used to simulate the flow of paste through the conical die depicted in Fig. 1. The finite element results are compared with the experimental results as a check on the validity and usefulness of the rheological constitutive equation. In addition, the flow simulation is used to predict the extrusion pressure as a function of the operating and die geometrical characteristics and to explore the relationship between the tensile strength of the extrudate and the degree of fibrillation. In this last task, the average structural parameter at the exit, $\bar{\xi}_{exit}$, is related with the experimental tensile strength for a range of the operating and die geometrical parameters.

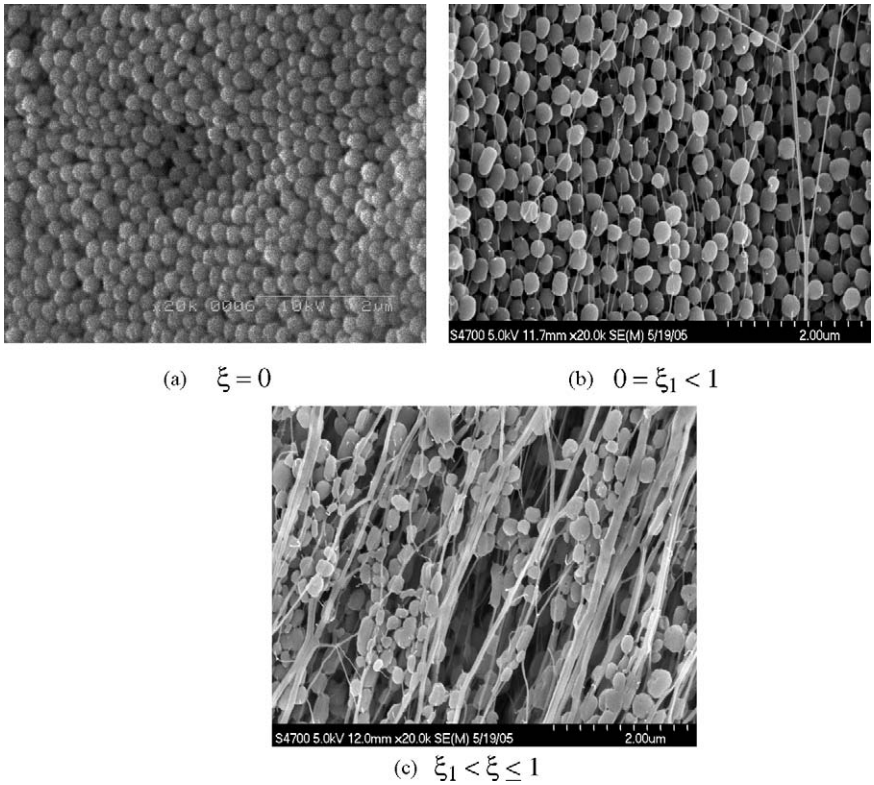

(a) $\xi = 0$ (b) $0 = \xi_1 < 1$

(c) $\xi_1 < \xi \leq 1$

Fig. 2. SEM micrographs of PTFE paste at various stages of the paste extrusion process: (a) before processing (nearly no-fibrillation), (b) during processing (partially fibrillated sample with small ξ), and (c) after processing (nearly fully fibrillated sample with larger ξ).

2. Theoretical modeling and numerical method

2.1. Governing equations

The steady-state mass and momentum conservation equations coupled with the rheological constitutive model are solved to simulate the flow of the PTFE paste. The axisymmetric r–z domain (Fig. 1) has been used to perform the simulations. The velocity field $\mathbf{v}$ is subject to the incompressibility constraint (small volume changes due to fibril formation that involve phase change are assumed to be small):

$$\nabla \cdot \mathbf{v} = 0. \tag{1}$$

Due to the high viscosity of the paste, the inertial terms in the momentum equation are neglected:

$$\nabla p - \nabla \cdot \boldsymbol{\tau} = 0, \tag{2}$$

where p is the pressure and $\boldsymbol{\tau}$ is the stress tensor, which depends on the structural parameter, ξ, through a constitutive equation developed below.

2.1.1. Constitutive equation

The rheology of the PTFE paste depends on the formation and evolution of a network of fibrils connecting PTFE polymer particles during the extrusion. To model this complex flow behavior, a rheological constitutive equation is proposed which explicitly accounts for the evolution of fibrils. Prior work has modeled flow induced structure formation in concentrated suspensions, polymer solutions and filled polymers as a combination of shear-thinning behavior at low shear rates and shear-thickening behavior at high shear rates [15,19,20]. A similar concept has been adopted in the present study to model the PTFE paste flow behavior. The rheology of the paste continuously changes as it flows through the conical sections. It starts as a two phase fluidlike system, an oversaturated suspension (Fig. 2a) and it ends as a highly fibrillated solidlike system. While the paste initially behaves as a shear-thinning fluid, after the appearance of fibrils in its structure, it behaves more and more as a shear-thickening fluid. Thus, it is assumed that the stress tensor consists of two contributions coming from the unfibrillated and fibrillated domains of the paste, represented, respectively by a shear-thinning and a shear-thickening viscous stress. The relative significance of the two contributions should depend on the structural parameter, ξ. Recall that the structural parameter, ξ is the percentage of the domains of the system that are fibrillated, and takes values between 0 and 1. Arguably, the rheological consequences of the fibrils may be modeled more accurately by elastic strain hardening rather than by shear-thickening. But the flow simulations would be much more involved.

Thus, the total viscous stress can be written in the following form:

$$\boldsymbol{\tau} = (1-\xi)\eta_1\dot{\boldsymbol{\gamma}} + \xi\eta_2\dot{\boldsymbol{\gamma}}, \tag{3}$$

where $\dot{\boldsymbol{\gamma}}$ is the rate of strain tensor, and η_1 and η_2 are the shear-thinning and shear-thickening viscosities that are expressed by a Carreau model [14]:

$$\eta_i = \eta_\infty + (\eta_{0i} - \eta_\infty)(1 + (\lambda_i\dot{\gamma})^2)^{(n_i-1)/2},$$

where $i=1$ refers to shear-thinning ($n_1<1$) and $i=2$ refers to shear-thickening ($n_2>1$). The values of parameters η_∞, η_{0i}, η_1 and λ_i are discussed and reported in the following section.

The creation of fibrils has been attributed to the unwinding of mechanically locked crystallites due to the extensional nature of the flow in the conical region of the die [2,5]. The extensional flow also causes elongation of newly formed fibrils which might also break depending on the total local Hencky strain. Therefore, both creation and breakage are possible. A kinetic model is proposed for the structural parameter, which is a balance of the fibrillated and unfibrillated domains of the paste and whose dynamics are controlled by the rates of creation and breakage:

$$\mathbf{v} \cdot \nabla\xi = f - g, \tag{4}$$

where f and g denote the rate of creation and elimination of fibrillated domains in the paste. These functions are given by

$$f(\dot{\gamma}, \psi) = \alpha\dot{\gamma}\sqrt{\psi}, \qquad g(\dot{\gamma}, \xi) = \beta\dot{\gamma}\xi, \tag{5}$$

where α and β are the dimensionless rate constants for fibril creation and breakage, both assumed to be 1 in our simulations; ψ the flow type parameter and $\dot{\gamma}$ is the magnitude of the strain rate tensor. The flow type parameter, ψ, indicates the relative strength of straining and rotation in a mixed flow [21–23]. Its magnitude ranges from -1 to 1 depending on the flow type as shown in Fig. 3. Since fibrils are mainly created due to elongation and never due to rotation, ψ is taken to vary only between 0 and 1. Negative values of ψ are reset to 0.

While the function f involves the formation of fibrils as unwinding of crystallites of neighboring particles, the function g represents their breakage. This is not to be taken as disappearance of the circular fibrils (see Fig. 2b and c) and reformation of perfect spherical particles. Broken fibrils do not contribute significantly to the overall pressure drop and to structural strength of the extrudate.

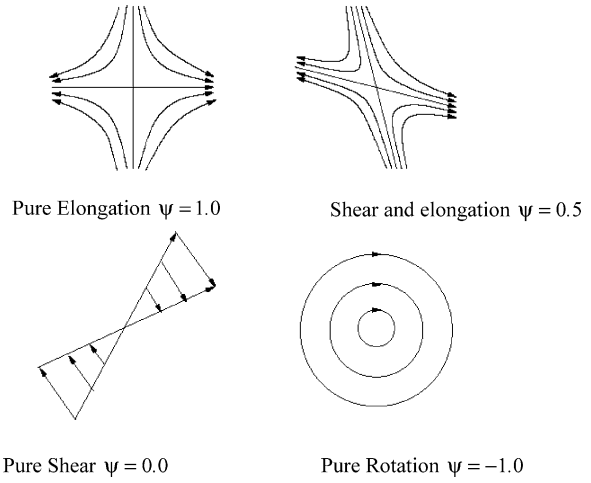

Fig. 3. Flow fields corresponding to different values of flow type parameters, ψ.

A final remark for the parameter ξ is as follows. It represents the percentage of the domains of the system that are fibrillated, and as such should take values between 0 and 1. This can be fixed by limiting the ratio of $\alpha/\beta \leq 1$ (note that both parameters have been assigned the value of 1). For example at steady-state conditions, Eq. (4) results $\xi = \alpha\sqrt{\psi}/\beta$, which essentially limits ξ to less than 1. Analytical solutions for one-dimensional axisymmetric flows where the velocity profile can be taken approximately know (fully developed) can be derived for Eq. (4) and these show that ξ is always less than 1. It should be noted that ξ can take the value of 1 in pure elongational flow, where ψ becomes 1.

2.1.2. Flow type parameter, ψ

The concept of the flow type parameter, ψ, has been used to account for the dependence of the structural parameter on the relative amount of straining and rotation in the flow field. As an example, a linear planar flow has a velocity field $\mathbf{v} = \boldsymbol{\Gamma} \cdot \mathbf{x}$, where $\boldsymbol{\Gamma}$ is the velocity gradient tensor [21–23]:

$$\boldsymbol{\Gamma} = \dot{\gamma} \begin{pmatrix} 0 & 1 \\ \psi & 0 \end{pmatrix}. \tag{6}$$

The flow of primary interest in our study is the strong flow for which $0 < \psi \leq 1$. Thus, for a planar flow, the largest eigenvalue of the velocity gradient tensor has the form of $\dot{\gamma}\sqrt{\psi}$ [21–23]. On the other hand the flow parameter ψ can also be written as

$$\psi = \frac{|\mathbf{D}| - |\mathbf{W}|}{|\mathbf{D}| + |\mathbf{W}|}, \tag{7}$$

where $\mathbf{D}$ and $\mathbf{W}$ denote the deformation and vorticity tensor, respectively. In the case of a axisymmetric flow, the velocity gradient tensor has a different form than Eq. (6), and its the largest eigenvalue is no longer equal to $\dot{\gamma}\sqrt{\psi}$. Nevertheless, we can still define ψ according to Eq. (7) and therefore, it retains the significance of a flow type parameter. It appears reasonable to use such a ψ in our kinetic Eq. (5). The magnitude of $\mathbf{D}$ and $\mathbf{W}$ in cylindrical coordinate can be written as follows:

$$|\mathbf{D}| = \sqrt{\left(\frac{\partial v_\mathrm{r}}{\partial r}\right)^2 + \left(\frac{v_\mathrm{r}}{r}\right)^2 + \left(\frac{\partial v_\mathrm{z}}{\partial z}\right)^2 + \frac{1}{2}\left(\frac{\partial v_\mathrm{r}}{\partial z} + \frac{\partial v_\mathrm{z}}{\partial r}\right)^2},$$

$$|\mathbf{W}| = \sqrt{\frac{1}{2}\left(\frac{\partial v_\mathrm{r}}{\partial z} - \frac{\partial v_\mathrm{z}}{\partial r}\right)^2}.$$

The flow type parameter controls the magnitude of structural parameter inside the flow domain with the maximum amount of fibrillation to occur at the center and much less at the die wall. This also ensures that the fibril creation and evolution mainly takes place inside the conical section; very little changes in fibril structure occur inside the die land where the flow becomes pure shear. This picture is supported by experimental evidence. This was confirmed by performing experiments with *L*/*D* ratios 0 and 20 [4,7,8]. Therefore, phenomenologically, the modeling concepts incorporated into our flow model agree well with the experimental observations. The agreement between the measured and calculated extrusion pressure, and the relationship between the structural parameter ξ and the dimensional strength of extrudate remain to be seen.

2.2. Boundary conditions

The boundary conditions used in the simulations are listed below:

(i) Inlet boundary conditions ($z = 0$): the numerical fully developed velocity profile for a shear-thinning Carreau fluid model has been imposed at the inlet with $v_\mathrm{r} = 0$. The no-fibrillation boundary condition is also assumed $\xi = 0$.

(ii) Outlet boundary conditions: the normal stress boundary condition and zero radial velocity are imposed:

$$n \cdot (-pI + \boldsymbol{\tau})n = -p_0; \quad v_\mathrm{r} = 0.$$

(iii) Slip boundary condition at the die wall: the Navier slip condition has been used at the die wall, which relates slip velocity with the wall shear stress, σ_w:

$$V_\mathrm{s} = C\sigma_\mathrm{w}.$$

where $C = 1.92$ m/MPa s. This value of C has been calculated from experimental data which will be discussed in the next subsection.

(iv) The axisymmetric boundary condition is used at $r = 0$:

$$v_\mathrm{r} = 0, \quad \frac{\partial v_z}{\partial r} = 0.$$

2.2.1. Slip boundary condition

No experimental data on the slip velocity of polymer pastes was available, and thus it was decided to perform a series of capillary extrusion experiments to determine the relation between slip velocity and wall stress using the Mooney analysis technique [10]. The paste was prepared using a high molecular weight PTFE resin (F-104) mixed with 38.8 vol.% Isopar® M as the lubricant; these are the same as those used by Ochoa and Hatzikiriakos [4]. The physical properties of isoparaffinic lubricant (Isopar® M) are listed in Table 1.

In capillary flow, the shear stress at the wall, $\boldsymbol{\sigma}_\mathrm{w}$, can be determined by correcting for the pressure losses associated with

Table 1
Physical properties of the Isopar® M lubricant used in the slip velocity measurements

Property	Isopar® M
Density at 25 °C (g/cm^3)	0.79
Surface tension at 25 °C (dyn/cm)	26.6
Vapour pressure at 38 °C (mmHg)	3.1
Viscosity at 25 °C (mPa s)	2.70
a (g^2 s^{-1} cm^{-5})	608.8

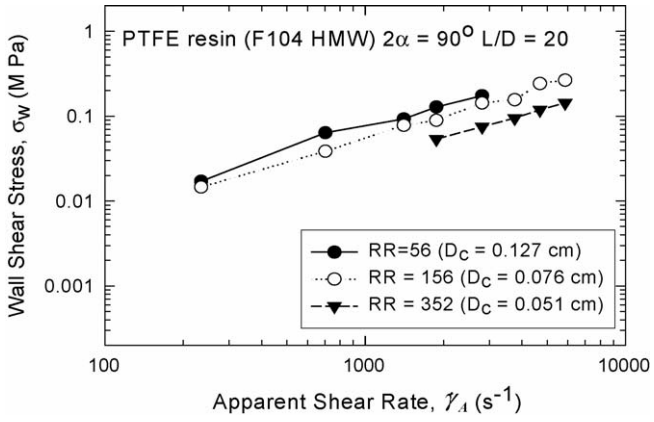

Fig. 4. The apparent flow curves of PTFE paste extruded through three dies having the same *L*/*D* ratio and different diameter.

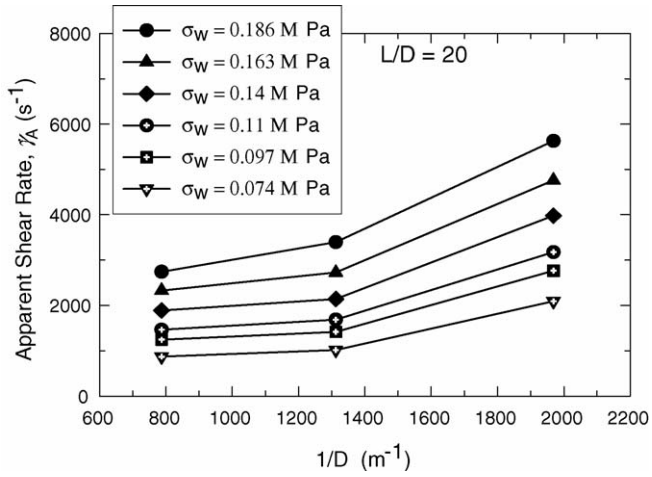

Fig. 5. Mooney plot based on the experimental data of Fig. 4 prepared to calculate the slip velocity. The shear stress values that correspond to individual lines at various shear stress values are also shown.

the end effects by using the Bagley correction [24,25]:

$$\sigma_w = \frac{\Delta p}{4(L/D + e)}, \tag{8}$$

where Δp is the total pressure drop over the capillary, L the length and D the diameter of the capillary, and "e" is the Bagley end correction in terms of an equivalent length associated with the end correction. The equivalent length can be determined either by extrapolating the Δp versus the L/D ratio curves to $L/D = 0$ or by performing experiments with a die having $L/D = 0$ [10]. The latter approach has been followed here to find the corrected pressure drop and therefore the wall shear stress. The apparent shear rate, $\dot{\gamma}_A$, is determined from $8\overline{V}/D$, where $\overline{V}$ is the average fluid velocity of the fluid, which is equal to the velocity of the piston in capillary extrusion.

To determine the slip velocity, capillary dies having the same length to diameter (*L*/*D*) ratios are used. Fig. 4 depicts the apparent flow curves of the paste for the same *L*/*D* ratio and different die land diameters. The analysis proposed by Mooney for fully developed, incompressible, isothermal, and laminar flow in circular tubes with a slip velocity of v_s at the wall yields:

$$\dot{\gamma}_A = \dot{\gamma}_{A,S}(\sigma_w) + \frac{8V_s}{D} \tag{9}$$

where $\dot{\gamma}_{A,S}$ is the apparent shear rate corrected for the effects of slip, solely a function of σ_w. Thus, a plot of the apparent shear rate, $\dot{\gamma}_A$, versus $1/D$ at constant σ_w values should result straight lines with slopes equal to $8v_s$ provided that the Mooney analysis is correct. This is done in Fig. 5. The individual data points do not fall on perfect straight lines, which might be due to experimental error. In spite of this, and since an approximate expression for the slip velocity is needed, the slopes of best fit straight lines passing through those points in Fig. 5 were calculated in order to determine the slip velocity as a function of σ_w. The plot of slip velocity, v_s, versus σ_w results a straight line with slope equal to 1.92 m/MPa s as shown in Fig. 6. This relation has been used in the simulations reported in the present study as a slip boundary condition at the die wall.

2.3. Finite element method

The equations of motion coupled with the proposed constitutive and structural parameter models were solved using the Galerkin finite element method. All simulations reported in this paper were performed by using the commercial finite element code FEMLAB 3.1. As the problem considered here is axisymmetric, two-dimensional meshes are used on the computational domain. These unstructured meshes comprise triangular elements of widely varying sizes, small and large elements being employed in regions where the rates of strain were large and small, respectively. The smallest elements are required near the die corners, especially the re-entrant corner. The total numbers of elements used are in the range of 3000–10,000. The corners are also rounded slightly to avoid geometrical singularity, and the local element size is chosen to be smaller than the fillet radius at the corner. The fillet radius is a small proportion of the capillary radius, and so the solution obtained from the analysis is expected to be close to the solution for a die with perfectly sharp

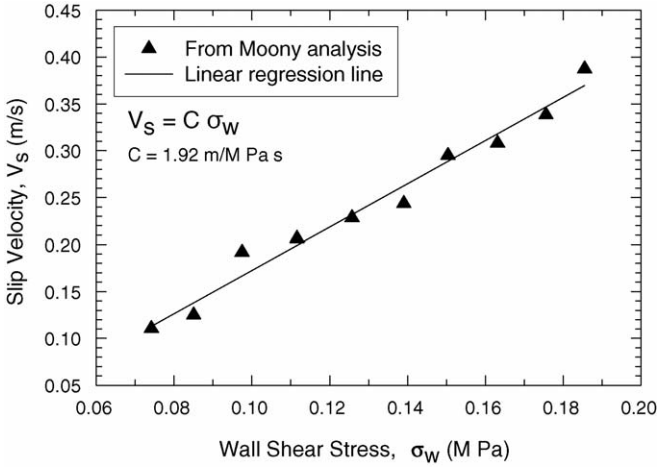

Fig. 6. The slip velocity, v_s, as a function of the wall shear stress, $\boldsymbol{\sigma}_w$ for a PTFE paste used in this work. A linear slip model seems adequate to capture the experimental results.

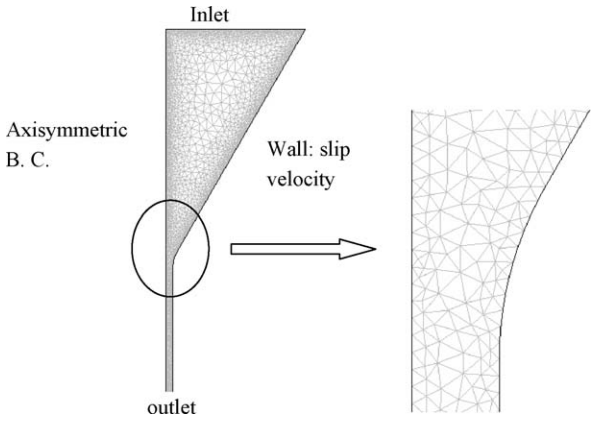

Fig. 7. Geometrical domain used for simulations with enlarged section of the rounded corner shown on the right side.

corners. Using meshes of the form shown in Fig. 7, the solutions were found to be insensitive to the number of mesh elements. The simulations are carried out for various die design parameters: the die reduction ratio, (RR $= D_b^2/D^2$), the die land length to diameter ratio (L/D) and die entrance angle (2α). Simulations are also carried out for different inlet flow rates that correspond to various apparent shear rate values, $\dot{\gamma}_A$. The run time of the simulations is in the range of 200–1000 s on Intel Pentium IV 2.8 GHz with 1 GB RAM machines.

3. Results and discussion

In this section, the simulation results are reported and compared with the experimental findings of Ochoa and Hatzikiriakos [4] for pastes prepared by mixing a high molecular weight PTFE (F-104) with 38.8 vol.% Isopar®.

To gain a better understanding of the structure of PTFE paste flow, typical velocity profiles at various axial location inside the conical die ($2\alpha = 90^\circ$ and $L/D = 20$) are plotted in Fig. 8. The x-axis in Fig. 8 is a dimensionless radial distance that is the radial distance normalized with the capillary radius at the corresponding axial location. The flow inside the conical section is mostly elongational (note the significant slip at the wall) and this essentially causes the formation of significant amount of fibrils (ξ continuously increases). As ξ increases, it causes an increase of the breakage term in Eq. (4). This in turn might cause a decrease in ξ mostly before the entrance to the die land. Flow in the die land is simple shear with significant slip and there the velocity profile soon attains 'almost' a fully developed shape. The true shear rate is very small and this essentially causes very small changes in the velocity profiles which are quite insignificant (see Fig. 8 where the three profiles in the die land coincide and they differ very little with the profile at the entrance to the die land).

The effect of the entrance angle on the evolution of fibrils has also been explored. As will be seen later, the non-monotonic variation of the extrusion pressure with entrance angle has been captured with the present model. All the experiments reported in this section are for a high molecular weight PTFE (F-104) resin mixed with 38.8 vol.% of Isopar® M as lubricant [4].

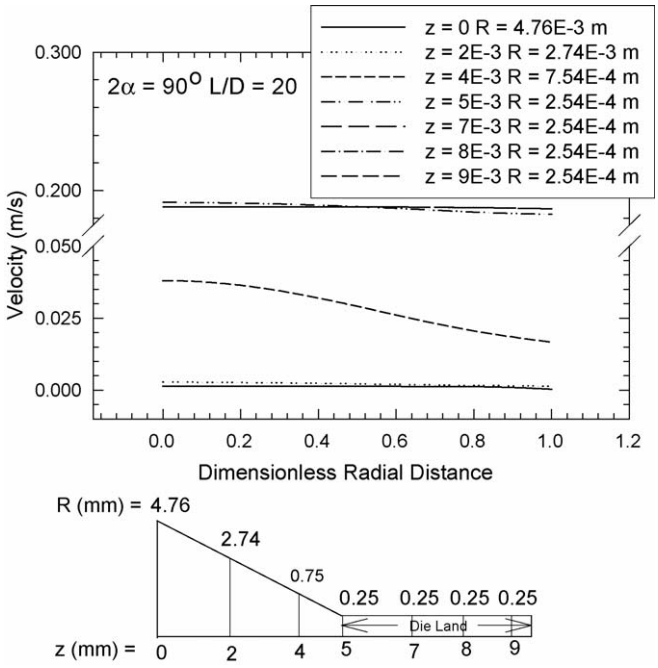

Fig. 8. Velocity profiles at various axial locations for a conical die having an entrance angle of 90°, and $L/D = 20$ at $\dot{\gamma}_A = 5869\,s^{-1}$.

3.1. Effect of die entrance angle

Simulations were performed for conical dies with RR = 352, $L/D = 20$ and various entrance angles in the range of $8^\circ \leq 2\alpha \leq 90^\circ$. The simulated dependence of the extrusion pressure on die entrance angle is shown in Fig. 9. The agreement between the predicted extrusion pressure and that obtained from the experimental analysis is very good. The parameters of Eq. (3) namely, η_∞, η_{0i}, η_i, and λ_i, are determined by a trial and error method until the best fit to the experimental data results. At first simulations were performed using parameter values arbitrarily chosen. Then depending on the difference between the calculated and experimental values new values were chosen. This is repeated till the best agreement between simulations and exper-

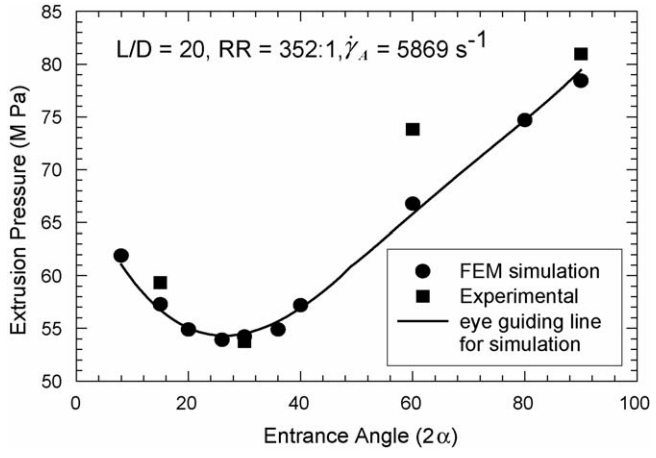

Fig. 9. The effect of die entrance angle on the extrusion pressure: comparison between experimental and simulation results.

Table 2
Parameters for the shear-thinning and the shear-thickening terms of Eq. (3)

Parameters	Shear-thinning	Shear-thickening
η_∞ (Pa s)	0	0
η_0 (Pa s)	4000	1600
λ (s^{-1})	0.3	1
n	0.5	1.3

imental values is obtained. The values of the parameters are reported in Table 2.

It can be seen that the initial decrease in the extrusion pressure with entrance angle is similar to the trend seen in capillary extrusion of polymer melts and other viscous liquids. This trend can be predicted by using the lubrication approximation assumption [12,26]. However, lubrication approximation is only valid for small entrance angles and use of this for larger entrance angles continues to predict decrease of the extrusion pressure monotonically. In fact, on the other hand, the extrusion pressure of PTFE increases significantly with increase of entrance angle beyond a certain critical value $2\alpha \approx 30^\circ$. Such a behavior is commonly observed in the extrusion of elastic solids (for example, see Horrobin and Nedderman [12] and the references therein). At very small entrance angle PTFE paste behaves mostly as a shear-thinning fluid with little fibrillation (small value of ξ) and this is captured by the present model. The flow type parameter, ψ, for small entrance angle is also close to zero and that ensures that the dominant contribution to the stress tensor comes from the shear-thinning part. As the entrance angle increases, the flow becomes more extensional and this has an impact on ψ and subsequently on ξ, with both dramatically increasing. The paste now becomes more solidlike and this can be modeled by the shear-thickening term included in the constitutive rheological model of Eq. (3). The dominant contribution at high entrance angles comes from the shear-thickening term which causes the significant increase in the extrusion pressure. It should be mentioned that our primary focus in modeling the PTFE paste extrusion process was to predict correctly this trend, that is the non-monotonic variation of extrusion pressure with entrance angle. Such an observation was initially countertuitive and mainly comes from the gradual change of the nature of the material from liquidlike to solidlike one.

Fig. 10 depicts the variation of the average structural parameter at the exit, $\bar{\xi}_{exit}$, with the entrance angle. It can be seen that the model predicts increase of the degree of fibrillation with increase of the entrance angle. This increase in the degree of fibrillation can now be related to the tensile strength of the extrudates, as more fibrils are expected to increase the dimensional stability of the extrudates [4]. Fig. 10 also plots the effect of the entrance angle on the tensile strengths of dried extrudates reported by Ochoa and Hatzikiriakos [4]. It can be seen that the tensile strength goes through a minimum with increase of the entrance angle. The initial decrease of tensile strength with entrance angle is certainly countertuitive and not predicted by the model in terms of $\bar{\xi}_{exit}$. It might be related to the initial decrease of the extrusion pressure with entrance angle. A higher pressure can mechanically lock crystallites of particle more tightly and

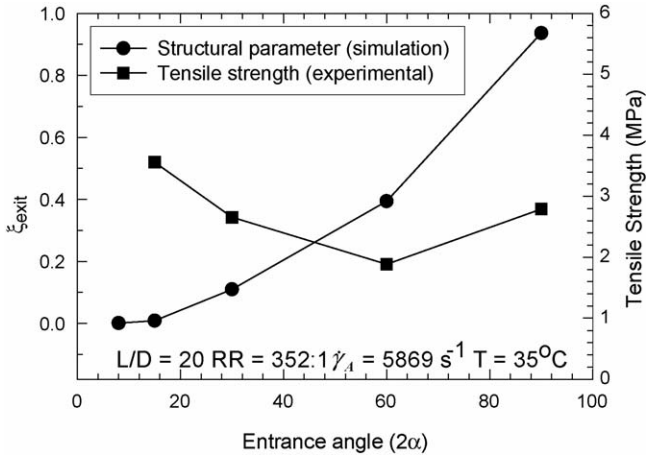

Fig. 10. The effect of die entrance angle on the cross-sectional average structural parameter at the exit, $\bar{\xi}_{exit}$ (from simulations) and the tensile strength of dried extrudates (from experiments).

this facilitates fibrillation. In our model the mechanism of fibrillation does not depend on local pressure and therefore such effects cannot be predicted.

3.2. Effect of apparent shear rate

Simulations were performed for various apparent shear rate values for a conical die having an entrance angle $2\alpha = 30^\circ$ and $L/D = 20$. The dependence of the extrusion pressure on apparent shear rate, $\dot{\gamma}_A$ ($\equiv 32Q/\pi D^3$) is shown in Fig. 11, where the agreement between the experimental and simulation results is excellent. It is noted again that the same parameters have been used for all comparisons with experimental results. The evolution of the structural parameter with apparent shear rate contributes to the monotonic increase of the extrusion pressure. Fig. 12 plots the average structural parameter at the exit $\bar{\xi}_{exit}$, as a function of the apparent shear rate, $\dot{\gamma}_A$. The simulation predicts a very small increase in fibrillation with increase in apparent shear rate, and this effect saturates quickly with increase in the apparent shear rate. An increase in $\dot{\gamma}_A$ causes an increase in the

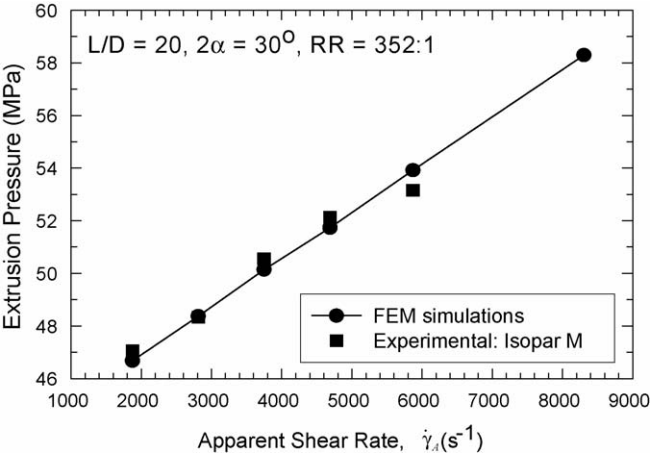

Fig. 11. The effect of apparent shear rate on the extrusion pressure of PTFE paste extrusion: comparison between experimental and simulation results.

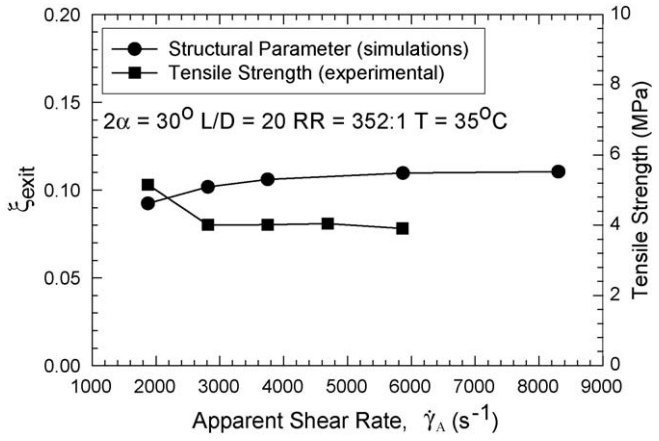

Fig. 12. The effect of apparent shear rate on the cross-sectional average structural parameter at the exit, $\bar{\xi}_{exit}$ (from simulations) and the tensile strength of dried extrudates (from experiments).

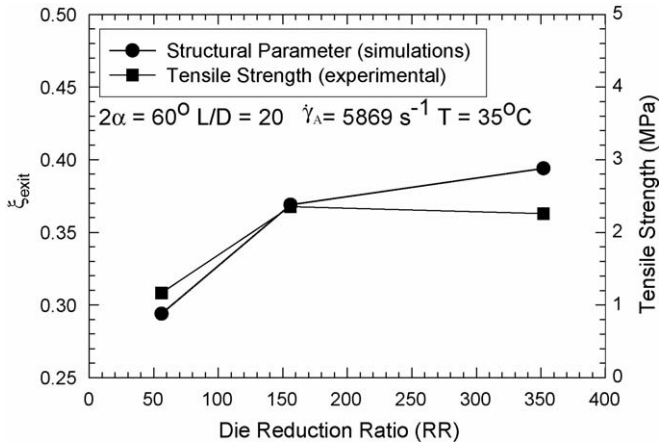

Fig. 14. The effect of die reduction ratio on the cross-sectional average structural parameter at the exit, $\bar{\xi}_{exit}$ (from simulations) and the tensile strength of dried extrudates (from experiments).

structural parameter ξ, and this in turn increases the rate of fibril breakage which results in slower increase of ξ at higher apparent shear rate. The experimental data of tensile strength show essentially no effect of the apparent shear rate on the tensile strength of the extruded paste (Fig. 12).

3.3. Effect of die reduction ratio

Simulations were performed for dies having $L/D = 20$, $2\alpha = 60^\circ$ and various reduction ratios in the range of $56 \leq RR \leq 352$. Fig. 13 depicts the effect of die reduction ratio on the extrusion pressure of the pastes. The agreement between the simulated and experimental dependence of extrusion pressure on die reduction ratio is again good. The extrusion pressure increases with the increase in the reduction ratio in a nonlinear fashion, which is captured by the simulated results. Fig. 14 shows that the structural parameter at the die exit $\bar{\xi}_{exit}$ increases with the reduction ratio. Experimental data show that the tensile strength also increases with the reduction ratio initially, but reaches a maximum at about RR = 156.

3.4. Effect of die length-to-diameter ratio

Simulations were performed for dies with RR = 352, $2\alpha = 90^\circ$ and several L/D ratios in the range of 0–40 at the apparent shear rate of 5869 s^{-1}. Fig. 15 plots the effect of the length-to-diameter ratio of the die, L/D, on the extrusion pressure of paste. The agreement between the simulated and experimental dependence of extrusion pressure on the L/D ratio is excellent. The extrusion pressure increases linearly with increase of the L/D ratio. Note that most of the resistance to flow is due to the conical zone. The pressure needed to extrude the polymer through the conical zone is about 60 MPa compared to an extra of about 25 MPa needed to extrude it through the straight section of $L/D = 40$ of the capillary die. The simulation results also predict an initial increase in the magnitude of $\bar{\xi}_{exit}$ with increase in L/D ratio as shown in Fig. 16. This effect saturates for $L/D > 10$. A similar trend is shown by the variation of the tensile strength with L/D ratio [4].

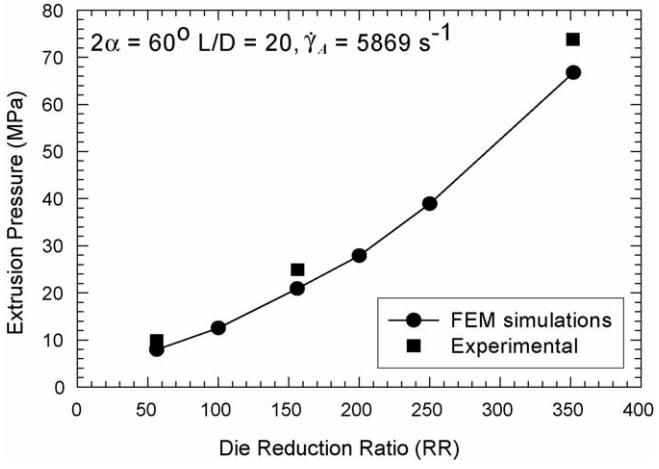

Fig. 13. Effect of die reduction ratio on extrusion pressure: comparison between experimental and simulation results.

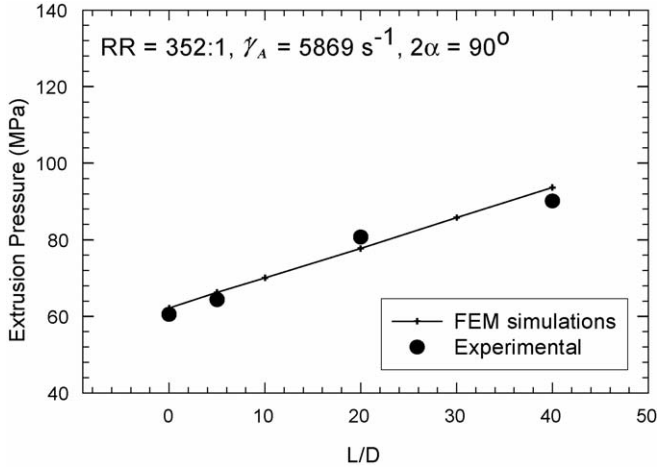

Fig. 15. The effect of length-to-diameter ratio (L/D) on the extrusion pressure: comparison between experimental and simulation results.

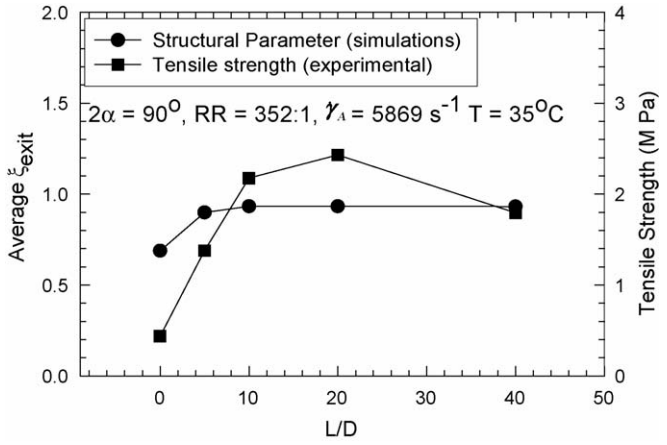

Fig. 16. The effect of die *L/D* ratio on average structural parameter at the exit, $\bar{\xi}_{exit}$ (from simulations) and the tensile strength of dried extrudates (from experiments).

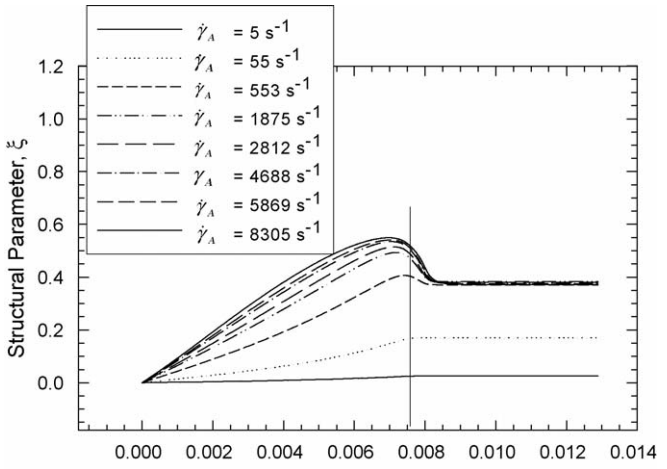

Fig. 18. Axial profiles of structural parameter along the centerline of a conical die having an entrance angle of 60° for various apparent shear rates indicated in the figure.

3.5. Structural parameter

The structural parameter is a quantitative measure of the degree of fibrillation in the sample during extrusion. Local axial variations of the structural parameter at various radial locations for a die having an entrance angle of 60° are shown in Fig. 17. Similar trends have been seen for other conical dies having other entrance angles. The structural parameter, ξ, increases from 0 at the entrance of the conical die and reaches a maximum before entering the die land. It can also be seen that once ξ relaxes to a constant level, it remains constant throughout the die land section.

Initially ξ increases as more and more fibrils are created due to the extensional flow in the conical die. As the end of the conical section is approached, the structural parameter, ξ increases further and this makes the rate of breakage higher than that of the creation. Overall this decreases the degree of fibrillation and as a result a maximum in the axial profile of ξ appears. The flow in the land region is simple shear with significant slip at the wall (see velocity profiles at Fig. 8) and therefore no additional fibrils are created. Furthermore, due to significant slip at the wall, the true shear rate is small; this causes the breakage rate to become negligible; as a result ξ in the land region remains essentially constant. Corresponding simulations under no-slip boundary condition causes ξ to decay to zero in the die land of the die, well before the exit.

Fig. 18 shows the effect of the apparent shear rate on the rate of creation and breakage of fibrils. For small values of the apparent shear rate, ξ increases till the exit of the conical section and remain constant thereafter instead of reaching maximum. Above a certain apparent shear rate value, $\dot{\gamma}_A$, of about 55 s^{-1}, the rate of breakage overcomes the rate of creation near the exit of the conical section, resulting the maximum in the axial profile of ξ.

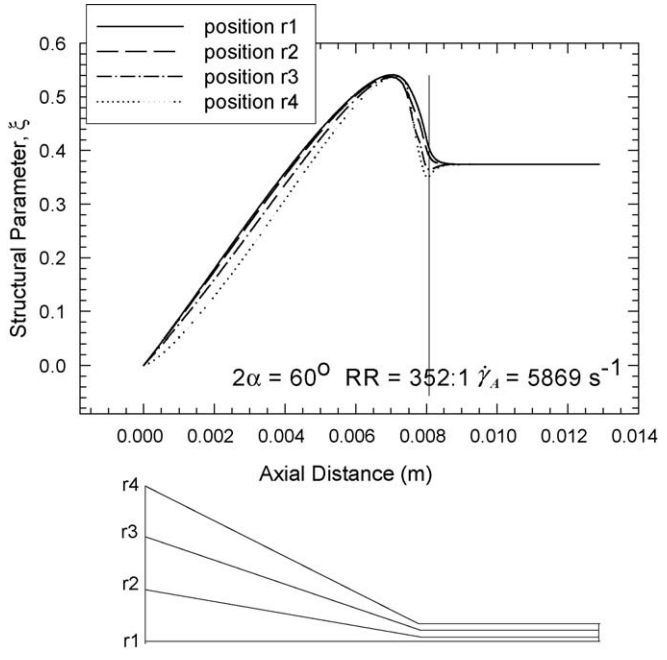

Fig. 17. Axial profiles of structural parameter at various radial locations for a conical die having an entrance angle of 60°.

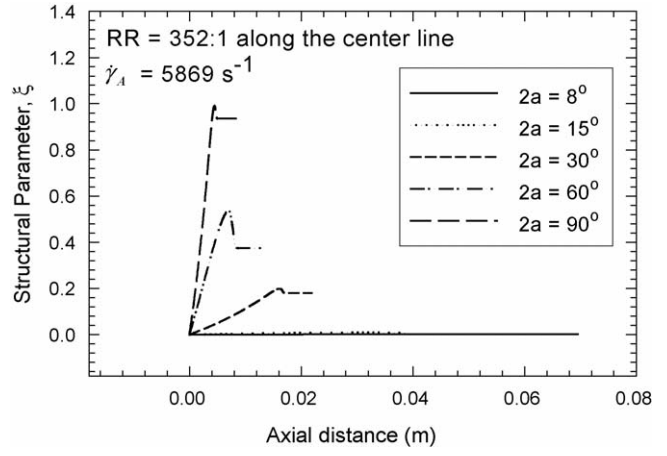

Fig. 19. Axial profiles of structural parameter along the centerline of conical dies having various entrance angles.

Fig. 19 shows the variation of structural parameter with axial distance along the centerline of dies having various entrance angles. The increase in the maximum value of structural parameter with entrance angle shows the increase in the degree of fibrillation. The increase in the structural parameter, ξ, with entrance angle is because of the increase in the elongational rate. The simulation results show that the creation of fibrils takes place inside the conical region with very little change in fibrillation in the die land region. This is agrees with the experimental observation by Ariawan et al. [7,8], and Ochoa and Hatzikiriakos [4].

4. Conclusions

In this work, finite element simulations of PTFE paste extrusion are presented in order to predict the dependence of extrusion pressure on apparent shear rate, die reduction ratio, die *L*/*D* ratio and die entrance angle. The rheological constitutive equation proposed, with the total stress comprising a shear-thinning term and a shear-thickening term, is capable of capturing the main features of the process as previously documented by experiments [4,7,8].

The PTFE paste has been treated as a shear-thinning fluid before the occurrence of fibrillation. The fibrils gradually turn the paste to exhibit more shear-thickening behavior. Change in the nature of the paste from a fluidlike behavior to a solidlike one, is implemented by the introduction of a microscopic structural parameter, ξ. An evolution equation has been developed for ξ based on the kinetic network theories [15–17]. The phenomena of fibril formation, evolution and breakage have been captured through this kinetic model.

Simulation results were found to be in excellent agreement with the experimental findings reported by Ochoa and Hatzikiriakos [4]. Based on this agreement it can be concluded that the proposed constitutive equation is suitable for modeling the behavior of the paste. In addition, the structural parameter, ξ, was related to the tensile strength of the pastes. The predicted effects of the die geometrical parameter and operating condition on the ξ are generally in agreement with the observed ones on the tensile strength.

Acknowledgements

This work has been supported financially by a grant from Daikin America. Dr. James Feng was also supported by the Donors of the Petroleum Research Fund, administered by the American Chemical Society, the NSERC and the Canada Research Chairs program. The simulations were performed on computers at the Institute of Applied Mathematics, University of British Columbia.

References

[1] T.A. Blanchet, Polytetrafluoroethylene, in: Handbook of Thermoplastics, Marcel Dekker Inc., New York, 1997, pp. 981–1000.
[2] S. Ebnesajjad, Fluoroplastics, vol. 1: Non-melt Processible Fluoroplastics, Plastics Design Library, William Andrew Corp., NY, 2000.
[3] C.A. Sperati, Physical Constants of Fluoropolymers, in: J. Brandrup, E.H. Immergut (Eds.), Polymer Handbook, John Wiley & Sons Inc., New York, 1989.
[4] I. Ochoa, S.G. Hatzikiriakos, Polytetrafluoroethylene paste preforming: viscosity and surface tension effects, Powder Technol. 146 (1/2) (2004) 73–83.
[5] S. Mazur, Paste extrusion of poly(tetrafluoroethylene) fine powders, in: M. Narkis, N. Rosenzweig (Eds.), Polymer Powder Technology, John Wiley & Sons Inc., New York, 1995, pp. 441–481.
[6] A.B. Ariawan, S. Ebnesajjad, S.G. Hatzikiriakos, Preforming behaviour of polytetrafluoroethylene paste, Powder Technol. 121 (2001) 249–258.
[7] A. B. Ariawan, Paste extrusion of polytetrafluoroethylene fine powder resins, Ph.D. Thesis, The University of British Columbia, Department of Chemical and Biological Engineering, 2002.
[8] A.B. Ariawan, S. Ebnesajjad, S.G. Hatzikiriakos, Paste extrusion of polytetrafluoroethylene (PTFE) fine powder resins, Can. J. Chem. Eng. 80 (2002) 1153–1165.
[9] A.B. Ariawan, S. Ebnesajjad, S.G. Hatzikiriakos, Properties of polytetrafluoroethylene (PTFE) paste extrudate, Polym. Eng. Sci. 42 (2002) 1247–1253.
[10] M. Mooney, Explicit formulas for slip and fluidity, J. Rheol. 2 (1931) 210–222.
[11] J.J. Benbow, J. Bridgwater, Paste Flow and Extrusion, Oxford University Press, NY, 1993.
[12] D.J. Horrobin, N.R. Nedderman, Die entry pressure drops in paste extrusion, Chem. Eng. Sci. 53 (1998) 3215–3225.
[13] R.B. Bird, O. Hassager, R.C. Armstrong, Dynamics of Polymer Liquids, vol. 1, 2nd ed., John Wiley & Sons Inc., New York, 1987.
[14] R.B. Bird, O. Hassager, R.C. Armstrong, C.F. Curtiss, Dynamics of Polymeric Liquids, vol. 2, Kinetic Theory, John Wiley & Sons Inc., New York, 1987.
[15] R.J. Jeyaseelan, A.J. Giacomin, Structural network theory for a filled polymer melt in large amplitude oscillatory shear, Polym. Gels Networks 3 (1995) 117–133.
[16] T.Y. Liu, D.S. Soong, M.C. Williams, Transient and steady rheology of polydisperse entangled melts: predictions of a kinetic network model and data comparisons, J. Polym. Sci.: Pl. Phys. Ed. 22 (1984) 1561–1587.
[17] S.G. Hatzikiriakos, D. Vlassopoulos, Brownian dynamics simulations of shear-thickening in dilute polymer solutions, Rheol. Acta 35 (1996) 274–287.
[18] A.I. Leonov, On the rheology of filled polymers, J. Rheol. 34 (7) (1990) 1039–1068.
[19] H.M. Laun, R. Bung, S. Hess, W. Loose, O. Hess, P. Linder, Rheological small angle neutron scattering investigation of shear induced particle structures of concentrated polymer dispersions submitted to plane Poiseulle and Couette flow, J. Rheol. 36 (4) (1992) 743–787.
[20] P.N. Dunlap, L.G. Leal, Dilute polystyrene solutions in extensional flows birefringence and flow modification, J. Non-Newton. Fluid Mech. 23 (1987) 5–48.
[21] G.G. Fuller, J.M. Rallison, R.L. Schmidt, L.G. Leal, The measurements of velocity gradients in laminar flow by homodyne light-scattering spectroscopy, J. Fluid Mech. 100 (3) (1980) 555–575.
[22] G.G. Fuller, L.G. Leal, Flow birefringence of dilute polymer solutions in two-dimensional flows, Rheol. Acta 19 (1980) 580–600.
[23] J.M. Dealy, K.F. Wissbrum, Melt Rheology and its Role in Plastics Processing: Theory and Application, Kluwer Academic Publisher, Amsterdam, 1990, pp. 305–307.
[24] C.S. Macosko, Rheology Principles, Measurements and Applications, VCH Publishers Inc., New York, 1994, pp. 244–247.
[25] G.R. Snelling, J.F. Lontz, Mechanism of lubricant-extrusion of Teflon® TFE-tetrafluoroethylene resins, J. Appl. Polym. Sci. III (1960) 257–265.